

Vacuum UV photoionization mass spectrometry of small polymers using jet cooling

M.S. de Vries, H.E. Hunziker *

IBM Research Division, Almaden Research Center, 650 Harry Road, San Jose, CA 95120, USA

Abstract

Many polymers with short chains and molecular weights up to several thousand atomic mass units can be transferred to the vapor phase whole by pulsed laser desorption, in contrast with the well-known, destructive ablation process encountered with long-chain, high-molecular-weight polymers. However, the vaporized whole polymers are hot and thus fragment extensively when photoionized. For their detection as molecular ions, it is necessary first to cool the vaporized polymers, which is accomplished by entraining them in an Ar jet expansion. Near-threshold, single-photon ionization at 125 nm (9.9 eV) was used in all cases and compared with 193 nm, two-photon ionization for polystyrene. Mass spectra showing oligomeric distributions for samples of poly(dimethylsiloxane), poly(ethylene oxide), poly(isoprene), poly(perfluorotrimethylene oxide) and polystyrene are reported. Application of the technique to samples of increasing average molecular weight shows that, as the chain length increases, thermal decomposition eventually predominates over vaporization. © 1997 Elsevier Science S.A.

Keywords: Small polymers; Jet cooling; Vacuum UV photoionization mass spectrometry

1. Introduction

There is now an arsenal of techniques capable of providing the mass spectra of whole polymers. A major subgroup of these new methods uses pulsed lasers to vaporize and ionize the high-molecular-weight material. Two important effects have been put to use in this approach to aid in the production of stable molecular ions: chemical ionization and matrix-assisted desorption. Many examples have been reported in which cationization with alkali ions, added to the polymer as salts, yields oligomeric mass distributions [1–4]. Hillenkamp and coworkers [5,6] originated and developed the matrix-assisted laser desorption/ionization (MALDI) technique, in which a low-molecular-weight organic matrix serves the dual function of entraining large molecules into the vapor phase without decomposition and ionizing them chemically usually by proton transfer.

Here we concern ourselves with the laser-induced vaporization of neat, low-molecular-weight polymers. In this case, without ionic dopants or ions created by laser-induced breakdown, there is no chemical ionization and the gas phase polymer molecules are neutral. Post-ionization is thus necessary to convert them into ions. Since this is usually performed by

photoionization with pulsed lasers, the procedure has also been called two-step laser mass spectrometry [7].

In this report, we address a problem which has limited the usefulness of laser desorption/post-ionization mass spectrometry. The desorbed molecules are hot and thus tend to fragment after ionization, unless the ions are very stable, as in the case of fullerenes or aromatic hydrocarbons [7,8]. A solution to this problem exists in the form of the laser desorption/jet cooling approach [9–11]. Cooling has already been used successfully to obtain the mass and optical spectra of small, aromatic polymers by two-photon ionization [12,13]. We show here that the combination of jet cooling with vacuum UV single-photon ionization near threshold makes it possible to obtain the parent mass spectra of small, aliphatic polymers. A somewhat similar approach was taken by Köster and Grottemeyer [14] to obtain the mass spectra of small, non-aromatic peptides. However, in their work, extensive fragmentation was observed.

2. Experimental details

Several previous studies have used vacuum UV post-ionization without cooling [15–17]. The vacuum UV pulses were generated by non-resonant third harmonic generation in phase-matched rare gas mixtures [18]. Because of its poten-

* Corresponding author.

tial for achieving higher vacuum UV fluences, we used resonance-enhanced four-wave mixing in Hg vapor instead, employing only a single, tunable dye laser at 625.70 nm to generate vacuum UV pulses at 125.14 nm [19]. This wavelength was also chosen because it is close to the ionization threshold of the higher paraffins. The experimental set-up is shown schematically in Fig. 1. A 30 cm achromatic lens was used to focus the fundamental and second harmonic inside the Hg vapor cell, which was operated at 140 °C and about 8 Torr Ar pressure. At the exit of the cell, a 5 cm diameter, 24.0 cm focal length (at 125 nm) LiF lens served a triple duty as cell window, focusing element and dispersing element for separating the vacuum UV from the pump beams. The biconical Hg cell was made from welded stainless steel parts, with Viton O-ring seals at the lens and window. For visible alignment, the LiF lens was replaced with a similar glass lens of 24 cm focal length at 625 nm. The holder for these lenses and that for the achromatic lens were laterally adjustable. By moving a vacuum UV mirror inside the vacuum chamber, the vacuum UV beam could be deflected onto a solar blind photodiode (Hamamatsu Type No. R1178, CsI cathode). From its nominal spectral response curve, the typical vacuum UV fluence was estimated to be 5×10^{11} photons per pulse.

Two different laser desorption/ionization set-ups were used in this work, one with and the other without jet cooling. The former has been described and characterized in detail previously [11]. Briefly, it consists of a pulsed nozzle, skimmer and reflectron time-of-flight (TOF) mass analyzer. Between the extraction grids of the analyzer, the molecular beam was crossed by a slightly focused 193 nm excimer laser beam which was used for two-photon ionization of aromatic chromophores. The 125 nm vacuum UV beam was intro-

duced along the jet axis and focused in the ionization volume, 110 cm from the LiF lens. Sample substances were deposited from dilute solutions onto 3 mm wide graphite bars which could be mounted through a load lock onto a translation stage in front of the jet orifice. A doubled Nd:YAG laser (532 nm) was used for desorption, with pulse energy densities of 10–100 mJ cm⁻² and a spot size of about 1 mm in diameter. Vaporization was caused by substrate heating only. Optimal injection of the vapor into the jet expansion occurred when the desorption spot was about 1 mm in front of and 0.5 mm below the nozzle, and the desorption laser was fired near the peak of the jet gas pulse. The pulsed valve was operated with Ar or Xe at a backing pressure of 8 atm.

The set-up without jet cooling involved a new laser microprobe ion source coupled to a reflectron TOF mass analyzer. An instrument described previously [20] was modified to pass the vacuum UV post-ionization beam closely (within 1 mm) over the desorption spot to maximize the ionization efficiency. An arrangement somewhat similar to that described by Odom and Schueler [21] was chosen, except that the ions were extracted through the blind spot of a 45° mirror rather than through the reflecting microscope objective. This has the considerable advantage of being able to work with a commercial reflecting objective.

Polymer samples were obtained from Daikin Industries (poly(perfluorotrimethylene oxide)), Polymer Laboratories Ltd. (poly(ethylene oxide), poly(isoprene) and polystyrene) and Aldrich (poly(dimethylsiloxane)). Most of these samples came characterized with M_p (GPC-peak molecular weight) or M_w (weight-average molecular weight) values. From the mass spectra, values of M_n (number-average molecular weight) and M_w were calculated for comparison with the

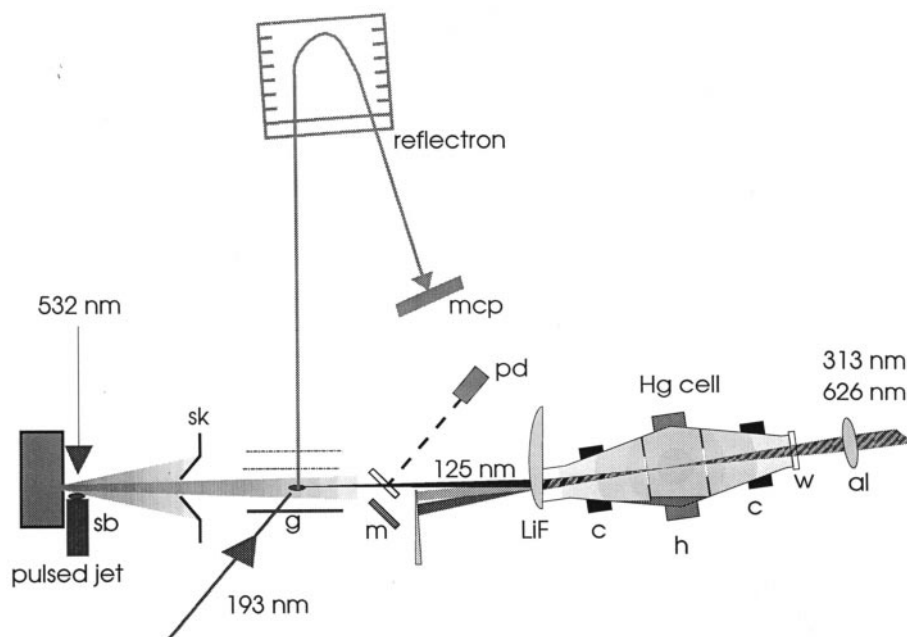


Fig. 1. Schematic diagram of the experimental set-up for laser desorption with jet cooling and post-ionization. Abbreviations: sb, sample bar; sk, skimmer; g, ion source grids; m, movable mirror; pd, photodiode; mcp, multichannel plate detector; LiF, plano-convex lithium fluoride lens; c, annular cooler; h, annular heater; w, fused silica window; al, achromatic lens.

nominal values. For these calculations, the peak amplitude of an oligomer was used to estimate its abundance, since the integrated peak area did not yield significantly different results.

3. Results

Initial experiments with *n*-paraffins from C₂₀ to C₄₀ showed that laser desorption in vacuum, followed by vacuum UV post-ionization, leads to almost complete fragmentation of the molecular ions. With short time delays between desorption and ionization (when sampling the hot portion of the desorption plume), the mass spectra obtained resemble standard 75 eV electron impact ionization spectra. With long delays, the spectra are weaker, but contain enhanced molecular ion signals. At fixed delay, the fragmentation increases with increasing desorption laser energy density. Gas phase molecules from room temperature sample evaporation, observed up to C₂₂, show much less fragmentation.

The effect of thermal excitation acquired during desorption is illustrated in Fig. 2 for a small perfluorotrimethylene oxide polymer with an aromatic end group. The positive ion fragments preferentially by losing the terminal phenoxy radical

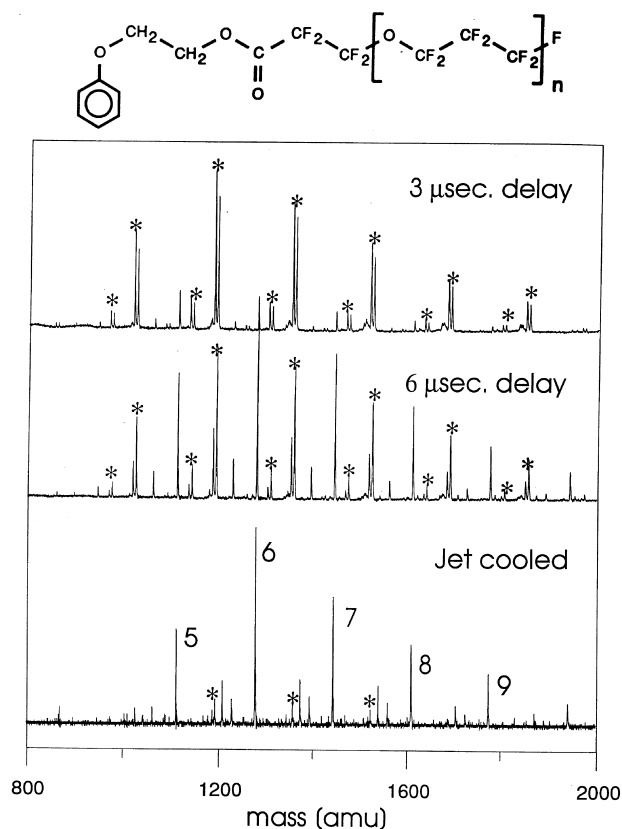


Fig. 2. Vacuum UV ionization mass spectra of a small perfluorotrimethylene oxide polymer (structure shown at the top). The top two traces were produced by desorption in vacuum, with the desorption/ionization delays indicated (average flight distance, approximately 1 mm). The bottom trace, with the molecular peaks labeled with the number of repeat units *n*, was measured with jet cooling. Asterisks mark the prompt/metastable fragment doublets.

(C₆H₅O, mass 93 amu). Prompt fragmentation produces a peak 93 amu below the parent, while slow fragmentation occurring in the first field-free region of the reflectron mass spectrometer gives rise to a metastable signal appearing about 6.5 amu above the prompt peak. These prompt/metastable fragment doublets are denoted by asterisks in Fig. 2. When the fast portion of the desorption plume is sampled at 3 μs delay, fragmentation is nearly complete, and more than half of it is prompt. Ionization of the slower portion at 6 μs delay produces a substantial parent signal, and the fragmentation is predominantly from metastable ions. The bottom trace of Fig. 2 shows the effect of jet cooling: fragmentation is almost completely eliminated. Minor peaks in this trace are due to a residue of metastable fragmentation, and to two modified forms of the main polymer which are present as impurities in the sample [13]. One of these is missing a CF₂ group (–50 amu peaks) and gives rise to the minor fragment doublets in the top two traces of Fig. 2. The other carries the phenoxy-terminated end group of the main polymer at both ends (–70 amu peaks); its fragments are not detected.

The effect of jet cooling is dramatic for high-boiling, saturated hydrocarbons. Fig. 3 shows the mass spectrum of squalane, a multiply branched C₃₀ paraffin, obtained with the jet/vacuum UV configuration. There is hardly any fragmentation at all; instead, clusters appear at multiples of the parent mass. When analyzing a mixture of unknowns, such cluster signals provide useful confirmation that the base masses are molecular ions and not fragments.

We applied the jet/vacuum UV technique to some readily available samples of small, aliphatic polymers. Fig. 4 shows the mass spectra of two different samples of poly(ethylene oxide). Panel B is a pure reference sample of nominal *M_p* = 1000 amu. Panel A is a laboratory detergent called Liqui-Nox (Alconox Inc.). Both spectra show an oligomeric distribution of parent ions. Using the oligomer peak heights as a measure of abundance, *M_n* = 840 amu and *M_w* = 880 amu were calculated for the reference sample, whose masses are consistent with the formula H–(O–CH₂–CH₂)_{*n*}–OH.

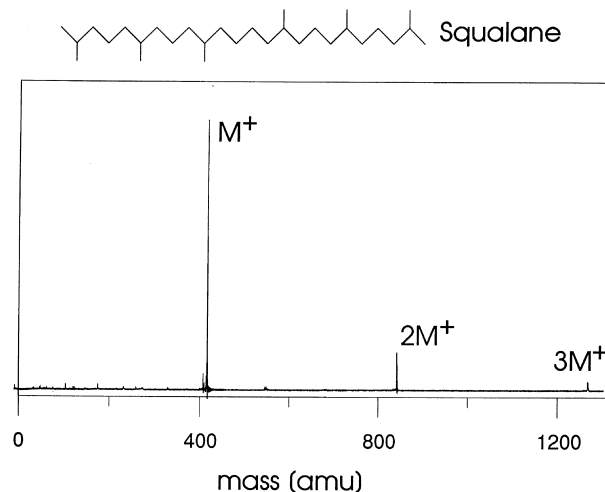


Fig. 3. Jet/vacuum UV mass spectrum of squalane. Signals at multiples of the parent mass are due to van der Waals' dimers and trimers.

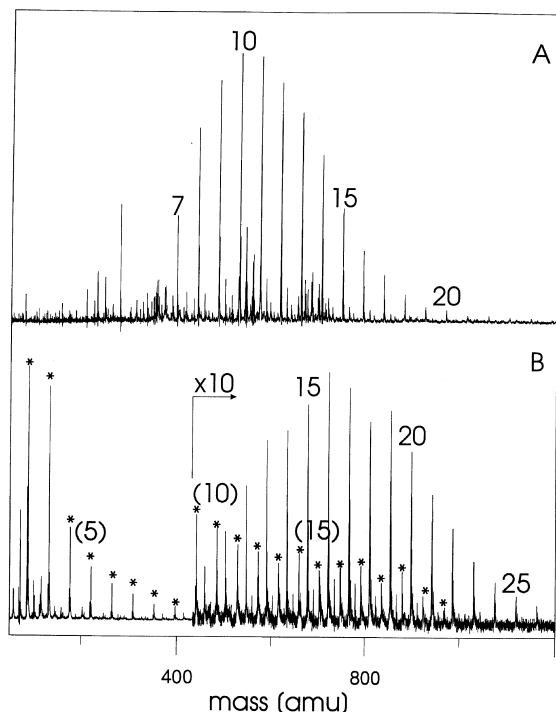


Fig. 4. Jet/vacuum UV mass spectra of poly(ethylene oxide) samples: (A) Liqui-Nox laboratory detergent; (B) reference sample with nominal $M_p = 1000$ amu; a fragment series in spectrum B is labeled with asterisks. The number n of ethylene oxide repeat units is given for some peaks (in parentheses for fragment series).

The spectrum of this sample also shows a distribution of low-molecular-weight fragments with masses $n \times 44$ amu whose abundance increases monotonically with decreasing weight. In addition, there is a prominent odd-mass fragment at 71 amu. The polymer in Liqui-Nox is shorter, and its mass values also conform to the formula $n \times 44$ amu. Since this is a detergent, the composition is probably $C_5H_{11}-(O-CH_2-CH_2)_n-OH$.

Fig. 5 shows the mass spectrum of a sample of poly(isoprene) with nominal $M_p = 1000$ amu. It corresponds to the structure $C_4H_9-(CH_2-C(CH_3)=CH-CH_2)_n-H$. From the peak heights, we calculate $M_n = 820$ amu and $M_w = 870$ amu. At the low mass end, this spectrum shows peaks for the isoprene monomer (68 amu) and dimer (136 amu).

For two types of polymer, we explored how the technique is limited by the molecular weight. The jet/vacuum UV mass spectra for three different samples of poly(dimethylsiloxane) with nominal M_w values of 800, 2000 and 6000 amu are shown in Fig. 6. In this case, the masses observed are all fragments missing one methyl group. The molecular ions corresponding to the structure $(CH_3)_3Si-(O-Si(CH_3)_2)_n-CH_3$ ($M = 88 + n \times 74$ amu) are not observed; instead, the spectrum shows the $M - 15$ amu ions. We also examined the cyclic tetramer and pentamer $(O-Si(CH_3)_2)_m$ ($m = 4$ and 5) and observed only the $M - 15$ amu ions. For the linear polymer samples shown in Fig. 6, the M_w (M_n) values determined from the mass spectra of the three samples were 950 (920), 1310 (1240) and 2150 (2010) amu respectively. There is

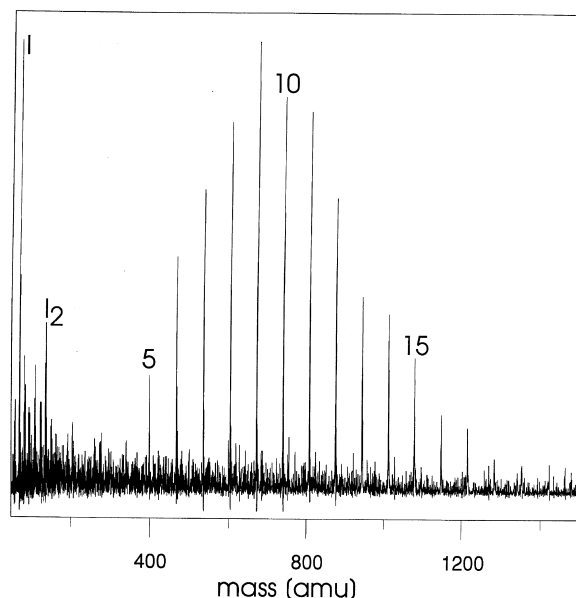


Fig. 5. Jet/vacuum UV mass spectrum of poly(isoprene) with nominal $M_p = 1000$ amu. The number n of isoprene repeat units is given for some peaks. I and I₂ refer to isoprene monomer and dimer.

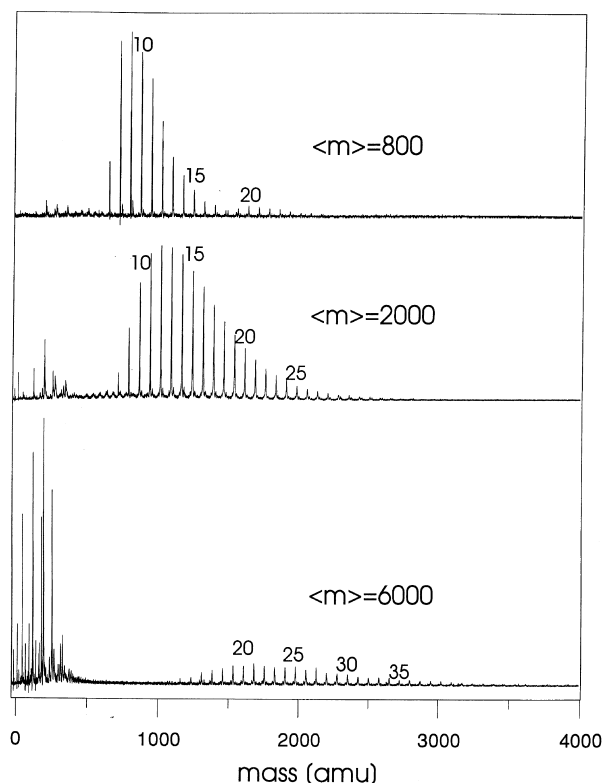


Fig. 6. Jet/vacuum UV mass spectra of three samples of poly(dimethylsiloxane) whose nominal M_p values are indicated in the figure. Numbers of repeat units n are indicated for some of the oligomer peaks which are all $(M - 15)$ amu masses.

clearly a lack of signals for higher oligomers, increasing with increasing M_w of the sample, and accompanied by an increasing proportion of low mass fragments in the mass spectrum.

The mass spectra of three polystyrene samples characterized by nominal M_p values of 950, 1300 and 4250 amu are

shown in Fig. 7. This is an aromatic polymer which can readily be ionized by two-photon ionization at 193 nm, and we used it to compare the ionization efficiencies of the two-photon and one-photon (125 nm) techniques. The sample composition corresponds to the structure $C_6H_5-(CH_2-CHP)_n-H$, where $P \equiv$ phenyl. For 193 nm ionization, the values of M_w (M_n) determined from the mass spectra were 910 (860), 1340 (1270) and 2120 (1830) amu respectively. For 125 nm ionization, the values were 780 (700) and 1220 (1150) amu, and the spectrum of the highest molecular weight sample was too weak to be evaluated. As for poly(dimethylsiloxane), there is a signal deficit for higher oligomers which increases with increasing average molecular weight of the sample and is accompanied by an increasing proportion of low mass fragments. The prominent fragment observed with 125 nm ionization is styrene; this was also detected by Feldmann et al. [15] as a photoablation product of polystyrene using 118.4 nm ionization. A comparison of the one-photon and two-photon ionization traces shows that the former exhibits a bias towards low mass when compared with the latter. Since the method of ionization is the only difference between these spectra, it follows that the ionization efficiency falls off more rapidly with molecular weight for the one-photon process.

4. Discussion

Our results show that laser desorption, combined with jet cooling and vacuum UV one-photon ionization, is capable of producing essentially fragment-free mass spectra of highly branched paraffins, such as squalane, as well as several types of small, aliphatic polymers. Cooling is essential; without it extensive fragmentation is observed. This is due to the high internal energy content of the vaporized molecules. As shown in the classic study by Steiner et al. [22], the photoionization cross-sections for fragmentation processes near threshold increase dramatically with temperature, whereas the cross-section for molecular ionization does not. Thus cooling stops fragmentation processes especially near the ionization threshold.

Cooling can only be effective if the ion has a stable ground state and fragmentation is thermally activated. This is not always the case. The complete absence of a molecular ion for all linear and cyclic poly(dimethylsiloxane) molecules shows that their molecular ions produced by vacuum UV ionization are intrinsically unstable. Judging from the ionization potential of $(CH_3)_3Si-O-Si(CH_3)_3$ (9.64 ± 0.01 eV [23]), the excess energy for vacuum UV ionization is small and similar to that of the paraffins, where cooling suppresses fragmentation completely.

We found that small polymers up to about $M_w = 1000$ amu are detected with only minor distortion of their mass distributions, whereas the spectra of samples with higher M_w are increasingly biased towards low mass oligomers. The onset of severe distortion depends somewhat on the type of poly-

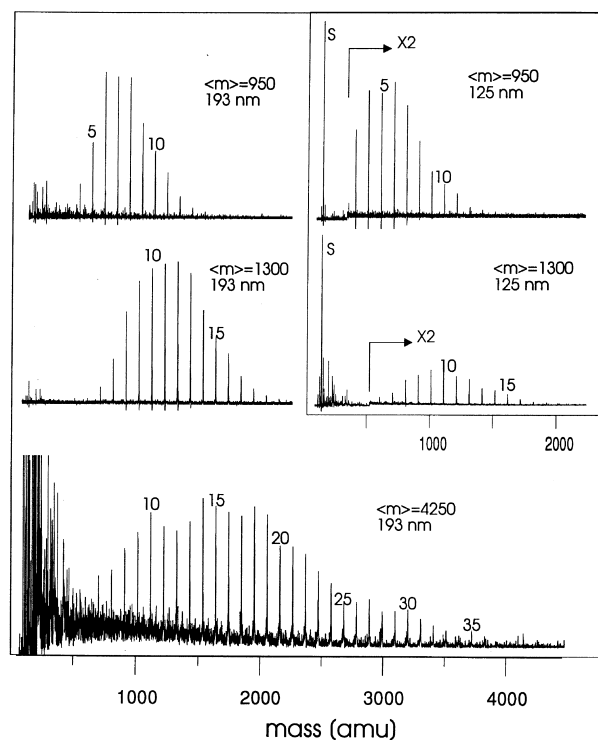


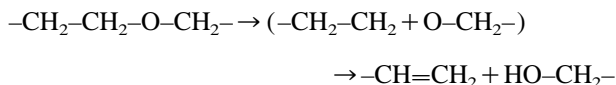
Fig. 7. One-photon (125 nm) and two-photon (193 nm) ionization mass spectra of three samples of polystyrene whose nominal M_p values are indicated in the figure. Some peaks are labeled with the number n of styrene repeat units. The low mass peak designated S in the 125 nm ionization spectra is styrene. Note the vertical scale change ($\times 2$) in these traces.

mer. We consider three causes for this effect: (1) preferential fragmentation of high mass ions; (2) competition between vaporization and thermal decomposition in the desorption step; (3) reduced ionization efficiency for high mass oligomers. Since we have no evidence for less efficient cooling of high mass neutrals, we regard cause (1) as unlikely. Schlag and Levine [24] have presented arguments and some evidence for cause (3). They proposed a mass dependence of the molecular ionization efficiency of the form $\exp(-M/M_0)^{3/2}$, where M is the molecular weight and M_0 is an empirical constant. This may account for part of the mass bias observed, but since the exponential falloff is steepest for the low masses, it cannot account for the increased distortion observed for $M > 1000$ amu. This increase is probably due to cause (2) which predominates in this mass range. For high mass molecules, dissociation becomes faster than vaporization. Desorption changes into ablation, which gives rise to an increased proportion of small fragments detected for samples of high average molecular weight.

It should be noted that our use of a graphite substrate and 532 nm light for desorption may favor thermal decomposition over vaporization when compared with IR laser-induced desorption. In the former, but not the latter, case, there is a high temperature transient at the substrate-sample interface. IR desorption combined with cationization has been used to detect higher oligomers of poly(ethylene oxide) than those reported here [4].

Even for $M < 1000$ amu, there appears to be relatively more efficient two-photon than one-photon ionization of the higher oligomers of polystyrene. Schlag et al. [25] reported a similar effect for small, aromatic peptides. They used identical total ionization energies, whereas in our case comparison is less direct because the energies are different (9.9 eV for one-photon ionization; 12.9 eV for two-photon ionization). This effect may be due to the increased oscillator strength (more chromophores) of higher oligomers in the first step of the two-photon process.

The poly(ethylene oxide) sample with nominal $M_p = 1000$ amu shows a fragment series with masses of $n \times 44$ amu ($n \geq 1$), monotonically increasing in intensity with decreasing mass (Fig. 4). This series fits none of the products found or intermediates postulated in thermal degradation studies [26,27], but is consistent with earlier laser desorption work in which the same series was observed in cationized form [4] and attributed to the random scission process



The vinyl-terminated product fits the observed fragment series. It must arise from pyrolysis because it is not a typical ether ion fragment [28] and can be detected by cationization [4]. It also does not occur in the spectrum of Fig. 4(A), where lower molecular weight and matrix effects (the presence of other low-molecular-weight mixture components) reduce pyrolysis. The discrepancy with slow thermal degradation presumably arises because the vinyl product is formed in a high activation energy unimolecular reaction which predominates under the conditions of laser desorption. A possible mechanism involves a concerted β -C–H hydrogen transfer [29]. In this case, the C–O bond scission shown in parentheses in the above reaction will be simultaneous with hydrogen transfer. The odd mass fragment observed at 71 amu may be the radical $\text{CH}_2-\text{CH}_2-\text{O}-\text{CH}=\text{CH}_2$ derived from the vinyl terminal by a simple C–O bond rupture.

Acknowledgements

We gratefully acknowledge the help of H.R. Wendt, D. Braichotte, K. Reihs and R. Baumann with the construction and characterization of the vacuum UV source. We also wish

to thank Daikin Industries for a sample of low-molecular-weight poly(perfluorotrimethylene oxide).

References

- [1] C.L. Wilkins, D.A. Weil, C.L.C. Yang, C.F. Ijames, *Anal. Chem.* 57 (1985) 520.
- [2] D.E. Mattern, D.M. Hercules, *Anal. Chem.* 57 (1985) 2041.
- [3] R.S. Brown, D.A. Weil, C.L. Wilkins, *Macromolecules* 19 (1986) 1255.
- [4] R.J. Cotter, J.P. Honovich, J.K. Olthoff, R.P. Lattimer, *Macromolecules* 19 (1986) 2996.
- [5] F. Hillenkamp, M. Karas, R.C. Beavis, B.T. Chait, *Anal. Chem.* 63 (1991) 1193A.
- [6] U. Bahr, A. Deppe, M. Karas, F. Hillenkamp, *Anal. Chem.* 64 (1992) 2866.
- [7] R. Zenobi, *Int. J. Mass Spectr. Ion Proc.* 145 (1995) 51.
- [8] K.R. Lykke, P. Wurz, D.H. Parker, M.J. Pellin, *Appl. Opt.* 32 (1993) 857.
- [9] H.v. Weyssenhoff, H.L. Selzle, E.W. Schlag, *Z. Naturforsch. Teil A* 40 (1985) 674.
- [10] R. Tembreull, D.M. Lubmann, *Appl. Spectrosc.* 41 (1987) 431.
- [11] G. Meijer, M.S. de Vries, H.E. Hunziker, H.R. Wendt, *Appl. Phys. B* 51 (1990) 395.
- [12] D.A. Lustig, D.M. Lubmann, *Int. J. Mass Spectr. Ion Proc.* 107 (1991) 265.
- [13] D.S. Anex, M.S. de Vries, A. Knebelkamp, J. Bargon, H.R. Wendt, H.E. Hunziker, *Int. J. Mass Spectr. Ion Proc.* 131 (1994) 319.
- [14] C. Köster, J. Grottemeyer, *Org. Mass Spectr.* 27 (1992) 463.
- [15] D. Feldmann, J. Kutzner, J. Laukemper, S. MacRobert, K.H. Welge, *Appl. Phys. B* 44 (1987) 81.
- [16] J.B. Pallix, U. Schuehle, C.H. Becker, D.L. Huestis, *Anal. Chem.* 61 (1989) 805.
- [17] S.E. Van Bramer, M.V. Johnston, *Appl. Spectrosc.* 46 (1992) 255.
- [18] R. Hilbig, R. Wallenstein, *IEEE J. Quantum Electron.* 17 (1981) 1566.
- [19] R. Hilbig, R. Wallenstein, *IEEE J. Quantum Electron.* 19 (1983) 1759.
- [20] M.S. de Vries, D.J. Elloway, H.R. Wendt, H.E. Hunziker, *Rev. Sci. Instrum.* 63 (1992) 3321.
- [21] R.W. Odom, B. Schueler, in: D.N. Lubman (Ed.), *Lasers and Mass Spectrometry*, Oxford University Press, New York, 1990, p. 122.
- [22] B. Steiner, C.F. Giese, M.G. Ingraham, *J. Chem. Phys.* 34 (1961) 189.
- [23] S.G. Lias, J.E. Bartmess, J.F. Liebman, J.L. Holmes, R.D. Levine, W.G. Mallard, *J. Phys. Chem. Ref. Data* 17 (Suppl. 1) (1988) 280.
- [24] E.W. Schlag, R.D. Levine, *J. Phys. Chem.* 96 (1992) 10 608.
- [25] E.W. Schlag, J. Grottemeyer, R.D. Levine, *Chem. Phys. Lett.* 190 (1992) 521.
- [26] N. Grassie, G.A. Perdomo Mendoza, *Polym. Degrad. Stab.* 9 (1984) 155.
- [27] E. Bortel, R. Lamot, *Makromol. Chem.* 178 (1977) 2617.
- [28] F.W. McLafferty, *Interpretation of Mass Spectra*, University Science Books, Mill Valley, CA, 1980, p. 209.
- [29] G. Allen, S.L. Aggarwal, S. Russo, *Comprehensive Polymer Science*, First Supplement, Pergamon, Oxford/New York/Seoul/Tokyo, 1992, p. 234.